



Regular article

A new beta titanium alloy system reinforced with superlattice intermetallic precipitates



Alexander J Knowles^{a, b}, Tea-Sung Jun^{a, c}, Ayan Bhowmik^a, Nicholas G Jones^b, T Ben Britton^a, Finn Giuliani^a, Howard J Stone^b, David Dye^a

^a Department of Materials, Imperial College, South Kensington, London SW7 2AZ, UK

^b Department of Materials Science and Metallurgy, University of Cambridge, Cambridge CB3 0F3, UK

^c Department of Mechanical Engineering, Incheon National University, 119 Academy-ro, Yeosu-go, Incheon 22012, South Korea

ARTICLE INFO

Article history:

Received 23 May 2017

Received in revised form 21 June 2017

Accepted 21 June 2017

Available online xxx

Keywords:

Titanium alloys

Precipitation

Microstructure

Mechanical properties

Dislocations

ABSTRACT

Titanium alloys traditionally lack a nm-scale intermetallic precipitate that can be exploited for age-hardening from solid solution. Here such a strengthening concept is developed in the Ti-Fe-Mo system, with it being found that a high temperature β (bcc A2) single-phase field for homogenisation can be obtained, which following ageing (750 °C/80 h) precipitated B2 TiFe <100 nm in size. The orientation relationship was found to be $\langle 100 \rangle_{A2} // \langle 100 \rangle_{B2}$, $\{100\}_{A2} // \{100\}_{B2}$, with a misfit of -6.1% . The alloy was found to be very hard ($HV_{0.5} = 6.4$ GPa) and strong ($\sigma_{y,0.2} = 1.9$ GPa) with a density of 6.68 g cm^{-3} . TEM observation and micropillar deformation showed that the precipitates resist dislocation cutting.

© 2017 Published by Elsevier Ltd on behalf of Acta Materialia Inc. All rights reserved.

Nickel based superalloys that comprise an fcc (A1) structured matrix reinforced with fcc superlattice precipitates (i.e. L1₂) are famed for their combination of strength, plasticity and creep resistance over a wide temperature range [1,2]. The microstructure concept of a disordered matrix with an ordered superlattice precipitate has also been applied to bcc (A2) materials [3,4]. For example, ferritic steels reinforced with B2 NiAl and/or L2₁ Ni₂TiAl precipitates have been found to have attractive creep performance [5,6]. The attempt to develop a similar strengthening concept in Ti-rich alloys has principally focused on the eutectic reaction between A2 Ti and B2 TiFe [7]. Developments of these alloys using ternary additions of Sn, Co [8] and Nb [9] have been successful at producing both higher strengths as well as increased ductility, which has been attributed to microstructural refinement.

An alternative microstructural production strategy to the eutectic reaction in the Ti-Fe binary system is the precipitation of B2 from within an A2 Ti matrix supersaturated with Fe, which may allow a nanoscale, rather than a microscale, microstructure to be produced.

This would allow for precipitation strengthening at a more appropriate lengthscale, enabling ductilisation strategies to be developed. The precipitation strategy would also allow for hot forgeability in the single phase field and therefore grain refinement and low cost net shaping in thick sections. In the Ti-Fe binary system the solubility for Fe within A2 Ti is known to change markedly with temperature [10,11]. However, Ti alloys rich in Fe are prone to ω formation [12], which can embrittle the material [13]. Ternary additions of Mo, which is a potent β stabiliser [14], >15 at.% [13,15] were envisaged to reduce the prevalence of athermal ω and so improve ductility. Studies have been made on phase equilibria in the ternary Ti-Fe-Mo system [16–18], with recent work demonstrating that A2 + B2 microstructures could be formed, which have high hardness, but also possessed an unavoidable micron scale intermetallic phase [19]. From the solvus position determined in previous studies [19,20] a new alloy has been designed that can be solution heat treated within the A2 single-phase field and subsequently aged at a lower temperature to form B2 precipitates within the A2 Ti matrix. Here, the microstructure of this new alloy with composition Ti-17Fe-23Mo (at.%) is discussed and its mechanical behaviour examined.

A 40 g sample was prepared by arc melting of pure (>99.9%) elements under Ar (see Fig. 1 in [21] for as-cast microstructure). Scanning electron microscopy (SEM) was performed on a Zeiss

* Corresponding author at: Department of Materials, Imperial College, South Kensington, London SW7 2AZ, UK.
E-mail address: a.knowles@ic.ac.uk (A.J. Knowles).

Auriga operated at 20 kV equipped for energy-dispersive X-ray spectrometry (EDX) as well as having a Bruker electron backscatter diffraction (EBSD) detector with ARGUS™ forescattered electron (FSE) detectors. The bulk composition of the alloy was evaluated by averaging five $200 \times 400 \mu\text{m}$ area measurements, at the top, bottom, centre and at either side of a section. It was found to be $(62.7 \pm 2.5)\text{Ti}$ – $(15.4 \pm 1.0)\text{Fe}$ – $(21.9 \pm 1.6)\text{Mo}$ (at.%), indicating a small amount of macrosegregation, while some casting porosity was also observed in the ingot.

After casting, the alloy's solidus was found to be 1180°C by differential scanning calorimetry (DSC) using a Netzsch 404 DSC. The alloy was solution heat treated in a quartz ampoule backfilled with Ar at 1170°C for 16 h and then water quenched, after which second phases were not observed in the SEM (see Fig. 1b in [21]). The alloy was then re-encapsulated and aged at 750°C for 80 h and then water quenched. The density, determined by the Archimedes method, was 6.7 g cm^{-3} . Grain sizes were determined by the linear intercept method [22] using FSE ARGUS™ images, from the top to bottom of the bar. The average grain size was found to be $160 \pm 30 \mu\text{m}$.

X-ray diffraction (XRD) was performed to determine the phases present in the alloy and their lattice parameters using $\text{Cu K}\alpha$ radiation on flat samples $\sim 8 \text{ mm}$ in diameter. Transmission electron microscopy (TEM) was performed using a JEOL 2100F microscope. TEM foils were prepared by mechanical thinning to $150 \mu\text{m}$ followed by electropolishing using 10 vol.% perchloric acid in methanol at -30°C and 18 V. Final thinning used a GATAN precision ion polishing system operated at 3 kV.

Microhardness indents using a 500 g load held for 10 s were made, averaging ten measurements. Macroscopic compression tests were performed on sub-sized 3 mm diameter, 5 mm high cylinders [23,24]. These were tested at a strain rate of 10^{-3} s^{-1} between SiC patterns lubricated with PTFE spray. Micropillars were prepared in a FEI Helios focused ion beam (FIB)-SEM, after Jun et al. [25]. These were square cross-section pillars $2 \mu\text{m}$ in width with height to width ratios of 1.9–2.6:1 [25]. The FIB micropillars were compressed *in situ* at a strain rate of 10^{-3} s^{-1} using an Alemnis nanoindenter in displacement control with a $10 \mu\text{m}$ diameter diamond punch tip in a FEI Quanta SEM.

After ageing ($750^\circ\text{C}/80 \text{ h}$), $29 \pm 2\%$ area fraction of fine lamellar precipitates could be observed with a width of $\sim 40 \text{ nm}$ ($41 \pm 14 \text{ nm}$, $n = 20$), spaced 70 nm apart ($68 \pm 20 \text{ nm}$, $n = 30$), Fig. 1a. The lamellae had darker backscattered electron (BSE) contrast when compared to the surrounding matrix, indicating a lower average Z. The XRD pattern collected from the alloy in the solution heat treated condition was found to contain A2 reflections with a lattice parameter of $3.14 \pm 0.01 \text{ \AA}$ (see Fig. 1b), with an additional peak noted at 42.5° . In the aged condition, reflections were observed from an A2 phase as well as a B2 phase, with lattice parameters of $3.18 \pm 0.01 \text{ \AA}$ and

$2.98 \pm 0.01 \text{ \AA}$ respectively. These represented a misfit $\delta a = -6.1\%$, where $\delta a = (a_{\text{precipitate}} - a_{\text{matrix}})/a_{\text{matrix}}$ [3]. In both conditions it was observed that each of the A2 reflections had shoulders at lower angles, which is indicative of the presence of ω phase [16]. In the aged alloy, the sole 42.5° peak in the solution heat treated condition may have been related to a low volume fraction of B2 or a reflection from the ω phase. TEM was employed to investigate further.

In the solution heat treated condition, bright field TEM and scanning TEM (STEM) imaging found no secondary features larger than 5 nm. Selected area diffraction patterns (SADPs) (with a 200 nm aperture) from a sample in the solution heated condition identified A2 reflections, Fig. 2a. Additional reflections consistent with incommensurate ω phase were observed, as previously reported in Ti-Fe alloys and Ti-Fe-Mo alloys [12,16]. No B2 reflections were observed, indicating that the 42.5° peak observed in XRD (Fig. 1b) was due to ω . However, B2 may have been sampled by XRD owing to macrosegregation, but not present in the small areas examined by TEM. Previous work on similar alloys has identified that ω occurs as $\sim 1 \text{ nm}$ domains formed on cooling [16]. SADPs (200nm aperture) collected in the aged condition are shown in Fig. 2b, with the A2 and B2 reflections identified, the B2 reflections corresponding to a smaller lattice parameter than the A2. An orientation relationship of $\langle 100 \rangle_{\text{A2}} // \langle 100 \rangle_{\text{B2}}$, $\{100\}_{\text{A2}} // \{100\}_{\text{B2}}$ was found. However, the axes of the B2 lamellae were not found to relate to fixed crystallographic directions. This suggests that the nucleation of the B2 precipitates is orientation dependent, but that their growth is not orientation confined. The microstructure and orientation relationship were suggestive of a (pseudo)spinodal decomposition or discontinuous precipitation. However, study of interrupted heat treatments would be required to confirm the formation reaction. The multiplicity of the higher order spots was due to double diffraction from the lamellae and matrix channels being of similar width to the foil thickness [26] (see Fig. 2 in [21]) as well as some foil bending. From the diffraction spots a misfit of -6.1% was found. Adjustment of the exposure time and contrast, Fig. 2c, identified additional diffuse reflections from the incommensurate ω phase. The lower intensity of the ω reflections when compared to the solution heat treated condition suggested that the aged condition may have a lower volume fraction of ω [27]. The streaking of the ω reflections indicates a structure change between the conditions, which may also influence their intensity [27].

High-angle annular dark-field (HAADF)-STEM imaging in the aged condition, Fig. 1d, indicated that the B2 precipitates had similar Ti content but were enriched in Fe and contained minimal Mo, Fig. 1e and f. This was consistent with near equilibrium compositions at 750°C of $(62.8 \pm 0.6)\text{Ti}$ – $(6.4 \pm 0.4)\text{Fe}$ – $(30.8 \pm 1.0)\text{Mo}$ (at.%) for A2 (Ti, Fe) and $(52.4 \pm 0.6)\text{Ti}$ – $(44.6 \pm 1)\text{Fe}$ – $(2.9 \pm 1.0)\text{Mo}$ for B2 TiFe [20]. The reduction in Fe and enrichment in Mo of the bcc (A2) matrix could be expected to lower the propensity for ω formation [13,27], as observed.

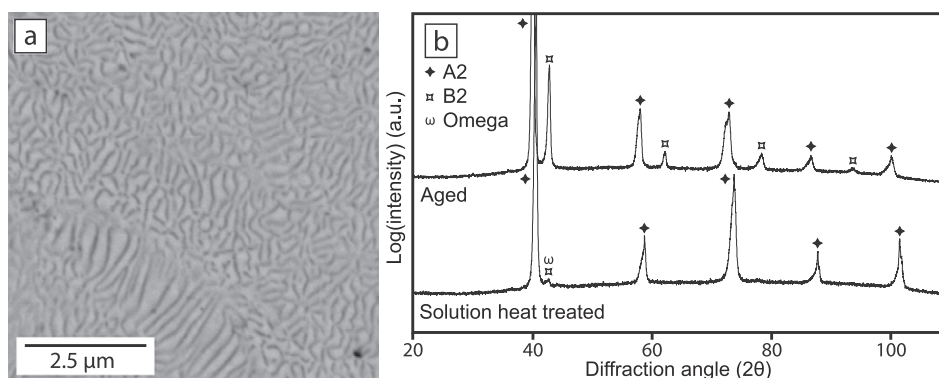


Fig. 1. (a) Microstructure observed by SEM BSE after ageing at 750°C for 80 h. (b) X-ray diffraction patterns obtained in the solution heat treated and aged condition ($\text{Cu K}\alpha$).

Download English Version:

<https://daneshyari.com/en/article/5443301>

Download Persian Version:

<https://daneshyari.com/article/5443301>

[Daneshyari.com](https://daneshyari.com)